# Coexistence and competition of local- and long-range polar orders in a ferroelectric relaxor

Guangyong Xu,[1] P. M. Gehring,[2] and G. Shirane[3]

[1]*Condensed Matter Physics and Materials Science Department, Brookhaven National Laboratory, Upton, New York 11973, USA*

[2]*NIST Center for Neutron Research, National Institute of Standards and Technology, Gaithersburg, Maryland 20899, USA*

[3]*Physics Department, Brookhaven National Laboratory, Upton, New York 11973, USA*

We have performed a series of neutron diffuse scattering measurements on a single crystal of the solid solution $Pb(Zn_{1/3}Nb_{2/3})O_3$ doped with 8% $PbTiO_3$, a relaxor compound with a Curie temperature $T_C \sim 450$ K, in an effort to study changes in local polar orders associated with the polar nanoregions (PNR) when the material enters the ferroelectric phase. The diffuse scattering intensity increases monotonically upon cooling in zero field, but the rate of increase varies dramatically around different Bragg peaks. These results can be explained by assuming that corresponding changes occur in the ratio of the optic and acoustic components of the atomic displacements within the PNR. Cooling in the presence of a modest electric field $\vec{E}$ oriented along the [111] direction alters the shape of diffuse scattering in reciprocal space, but does not eliminate the scattering as would be expected in the case of a classic ferroelectric material. This suggests that a field-induced redistribution of the PNR has taken place.

## I. INTRODUCTION

Lead perovskite relaxor systems such as $Pb(Zn_{1/3}Nb_{2/3})O_3$ (PZN) and $Pb(Mg_{1/3}Nb_{2/3})O_3$ (PMN) have been the focus of intense scientific scrutiny in recent years because they display exceptionally strong dielectric and piezoelectric properties.[1] These systems are marked by a strong, frequency-dependent dielectric permittivity that exhibits relaxation processes on many different time scales. This relaxational character has been attributed to the presence of small-scale regions of the lattice that possess randomly oriented, local polarizations, or "polar nanoregions" (PNR), which first appear at a temperature $T_d$, often referred to as the Burns temperature.[2] In PMN, for example, $T_d$ ($\sim 650$ K) lies a few hundred degrees above $T_m$, the temperature at which the dielectric permittivity is largest. Neutron scattering studies by Naberezhnov *et al.* have demonstrated the onset of strong diffuse scattering in PMN near $T_d$, thus indicating a strong link with the PNR. These polar nanoregions, or PNR, are believed to be several nanometers in size, grow with cooling, and are widely viewed to play important roles in determining relaxor properties.[3] For this reason we have undertaken a detailed study of the PNR properties using neutron diffuse scattering techniques.

Diffuse scattering is very sensitive to local inhomogeneities and short-range order in solid materials. It is thus an extremely powerful tool with which to study the structure of the PNR. Neutron and x-ray elastic diffuse scattering measurements on relaxor systems can provide important information about the size, shape, and polarization of the PNR. The data collected by Vakhrushev *et al.*[4] on the diffuse scattering intensity measured along directions transverse to the wave vector $\vec{Q}$ near many Bragg peaks in PMN provided the first quantitative study of the relative magnitudes of the atomic displacements (polarizations) within the PNR. In a subsequent study by Hirota *et al.*[5] the authors proposed the concept of the uniform phase shift, whereby the atomic displacements responsible for the PNR could be decomposed

into two components: an acoustic term that corresponds to a uniform shift of the entire PNR relative to the surrounding lattice, and an optic term that results from the condensation of a transverse optic (TO) phonon. Two other important features of the PNR are the directions of the polarizations and the shape of the PNR. These issues have also been extensively studied by diffuse scattering and other techniques.[6–12] Recently, Xu *et al.*[13] studied the three-dimensional diffuse scattering distribution in single crystals of PZN and its derivatives. These authors found that the diffuse scattering consists of six $\langle 110 \rangle$ rods. A model was proposed where $\langle 1\bar{1}0 \rangle$-type polarizations are correlated in $\{110\}$ planes, thus implying a "pancake" shape for the PNR with polarizations that lie in-plane.

Of course, with diffuse scattering measurements, it is not always easy to distinguish subtle differences in the local structure. In other words, are the PNR nanometer sized polar domains with well-defined boundaries; or local polar fields with short-range correlations? The former correspond to a square-type polar correlation, while the latter can be described with a gradually decaying, e.g., exponentially decaying correlation function with a certain length scale. In reality, the situation may lie somewhere in between. In other words, there could be "core" PNR regions around which the nearby lattice is slightly distorted. In this case the square-type correlation function should extend into the surrounding lattice with a decaying form. If the "core" PNR are large compared to the nearby distortion, we recover the former case; if the "core" PNR are small and the decaying distortion dominates, then we are close to the latter case. In both cases, local polar moments due to optic type atomic displacements exist in the system, as proposed by Burns and Dacol in their original PNR picture; and both can result in very similar diffuse scattering line shapes in the reciprocal space. In this paper, we are measuring the average effect of these local distortions, and do not attempt to make such a distinction. For simplicity, the term "PNR" is used throughout the paper. And when the "size" or "shape" of the PNR is concerned, they can be

viewed alternatively as length scales describing the local polar field (instead of the size of a well-defined nanoregion).

Considered by many researchers to be precursors to the ferroelectric phase transition, the PNR were expected to coalign or form much larger ferroelectric domains when the system is driven into a ferroelectric phase, either by cooling or by application of an external dc electric field. However diffuse scattering measurements have provided little such indication. Upon cooling in zero field, the diffuse scattering intensities increase monotonically in both PZN (Ref. 14) and PMN (Ref. 6) while the shape of the scattering remains the same, suggesting that the PNR persist at low temperatures. The effects of an external dc field on the diffuse scattering are more complicated; some studies[15,16] show a partial suppression of the diffuse scattering measured along the [110] and [001] directions, while more recent work[17,18] indicates that a redistribution of the PNR takes place when the sample is subjected to an external field oriented along the [111] direction. These studies indicate that in relaxor systems, that local- and long-range polar orders coexist and compete with each other.

The unit cells of pure PZN (Refs. 19 and 20) and PMN (Refs. 21 and 22) remain cubic when cooled in zero field; thus neither compound exhibits long-range ferroelectric order at low temperature. However, doping with $PbTiO_3$ (PT) to form the solid solutions PZN-$x$PT and PMN-$x$PT gradually suppresses the relaxor character and establishes a ferroelectric phase.[23] By increasing the PT content each system can be driven across a morphotropic phase boundary (MPB)[24–26] where a more conventional ferroelectric phase[27,28] is achieved. In this paper, we report neutron diffuse scattering measurements on PZN-8%PT, which does undergo a ferroelectric phase transition upon zero-field cooling. The low temperature phase has a rhombohedral structure with $\langle 111 \rangle$ type polarizations. Being on the relaxor side of the phase diagram, PZN-8%PT also exhibits relaxor properties and strong diffuse scattering.[13,16,17] The 8%PT content is also the composition at which the piezoelectric response is maximum,[24] thus making the PZN-8%PT compound a particularly interesting choice of system in which to study the PNR in a ferroelectric state.

We have studied how the diffuse scattering changes when PZN-8%PT is cooled into the ferroelectric phase under (i) zero field and (ii) an external field oriented along the [111] direction. The zero-field-cooling (ZFC) data show that the diffuse scattering has the same shape in the high temperature paraelectric and low temperature ferroelectric phases. The observed increase in total diffuse scattering intensity on cooling indicates a corresponding growth in the total PNR volume, or an increase in the PNR polarization, or both. However, there is a change in the ratio of the acoustic and optic components of the atomic displacements in the PNR. Specifically, the acoustic component of the atomic shift (uniform shift) in the PNR grows with decreasing temperature, which suggests an enhancement of local strain-type deformation takes place in the low temperature phase. After field cooling (FC), a clear redistribution of the diffuse scattering intensity is observed around all Bragg peaks, while the total (integrated) diffuse scattering intensity appears to be conserved, i.e., is at least equal to that in the ZFC case.

## II. EXPERIMENT

The PZN-8%PT single crystal used in this study is rectangular in shape, having dimensions of $5 \times 5 \times 3$ mm$^3$ with 111, $\bar{2}$11, and $0\bar{1}$1 surfaces, and was provided by commercial sources. Cr/Au electrodes were sputtered onto the top and bottom 111 crystal surfaces. This is the same crystal that was used in Ref. 17, which reported structural transitions from a cubic to tetragonal phase at $T_C \approx 440$ K, and then to a rhombohedral phase at $T_{C2} \approx 340$ K in zero field. Upon cooling in a moderate electric field of $E = 2$ kV/cm oriented along the [111] direction, the value of $T_C \approx 460$ K, while $T_{C2} \approx 340$ K does not change.

The neutron diffuse scattering measurements were performed with the BT9 triple-axis spectrometer located at the NIST Center for Neutron Research. The measurements were made using a fixed incident neutron energy $E_i$ of 14.7 meV, obtained from the (002) Bragg reflection of a highly oriented pyrolytic graphic (HOPG) monochromator, and horizontal beam collimations of 40′-40′-S-40′-80′ (S represents sample). The (002) reflection of an HOPG analyzer was used to select the energy of the scattered neutron beam. Two PG filters were placed before and after the sample to reduce the scattering from higher order reflections. Data were taken in the ($HKK$) scattering plane, defined by the two primary vectors [100] and [011], with the [111] electric field direction lying in the plane and the $0\bar{1}$1 crystal surface pointing vertically. All measurements were performed while cooling, starting from 550 K so that all residual (poling) effects are removed.

## III. RESULTS AND DISCUSSION

Previous measurements[17] have confirmed that the diffuse scattering intensities in PZN-8%PT form "butterfly" shaped patterns in zero field in the ($HKK$) scattering plane; this is shown schematically in Fig. 1(a). These butterfly patterns are in fact the result of the tails of out-of-plane $\langle 110 \rangle$ rods of diffuse scattering intensity, which are visible because of the nonzero instrumental out-of-plane wave vector ($q$) resolution. The "/"-shaped wing of the butterfly pattern measures the tails of diffuse rods oriented along the [110] and [101] directions, which arise from PNR having polarizations pointing along the [1$\bar{1}$0] and [10$\bar{1}$] directions; the "\"-shaped wing measures the tails of diffuse rods oriented along the [1$\bar{1}$0] and [10$\bar{1}$] directions, which arise from PNR having polarizations pointing along the [110] and [101] directions. An efficient way to monitor changes in the diffuse scattering is to perform linear $q$-scans in reciprocal space that are offset from the Bragg peak, as shown by the (red) arrows in Fig. 1. These linear scans have the advantage of being able to monitor the intensity changes in both the "/" and "\" wings of the butterfly pattern, which would not be possible with a (transverse) linear scan that cut across the Bragg peak itself.

Some of these linear scans are plotted in Fig. 2. We note that the linear scans near (300) [measured along $(2.9, K, K)$] and (200) [measured along $(2.1, K, K)$] produce a double-peak profile because the diffuse scattering intensity peaks at
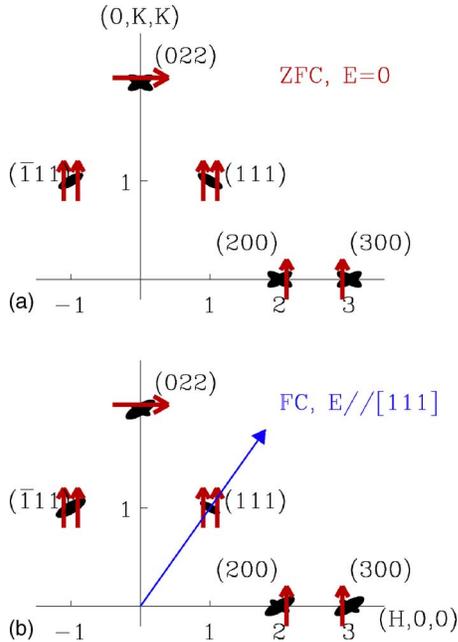
FIG. 1. (Color online) A schematic of the diffuse scattering intensity distribution in PZN-8%PT measured in the $(HKK)$ scattering plane around the (200), (300), (111), ($\bar{1}$11), and (022) Bragg peaks at 300 K after (a) zero-field cooling and (b) field cooling with $E=2$ kV/cm along [111]. The arrows indicate the linear scans performed in our measurements.

each wing of the butterfly pattern. By contrast the scans near (111) [measured along $(0.9,K,K)$] and ($\bar{1}$11) [measured along $(-0.9,K,K)$] only have one peak. This agrees well with the polarization analysis; the "/" wing comes from those PNR with polarizations perpendicular to [111], and thus is not observed around the (111) Bragg peak; neither is the "\" wing observed around the ($\bar{1}$11) peak.

In the following section, we study the change of the diffuse scattering intensity profiles when the system is driven into a ferroelectric phase by ZFC (Sec. III A) and FC (Sec. III B).

### A. Temperature effects

Upon ZFC from 500 K to 300 K, i.e., below $T_c$ the diffuse scattering intensities measured around all Bragg peaks increases. However, the rates of increase are very different. The diffuse scattering intensities around the (300) peak increase slightly from 500 K to 300 K, while those around the (200) peak grow by almost a factor of 2. Similar behavior was also observed in the relaxor system PMN, where the diffuse scattering intensities around (200) peak increase much faster with cooling than do those measured around the (300) peak.[29] In order to understand this change in the relative diffuse scattering intensities across different Bragg peaks, we first consider the various factors that determine the diffuse scattering intensities observed in PZN-8%PT.

Diffuse scattering refers to the relatively weak intensity that decorates broad regions of reciprocal space around different Bragg peaks. One source of this scattering arises from
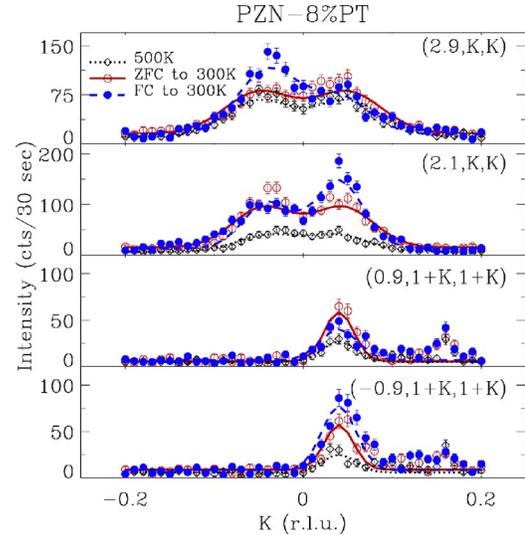


FIG. 2. (Color online) Diffuse intensity linear profiles, measured along the [011] direction around the (300), (200), (111), and ($\bar{1}$11) peaks, are shown from top to bottom, respectively. The lines through the data are fits to Gaussian functions of the reduced wave vector $q$ and are merely guides to the eye. The weak peaks in the (111) and ($\bar{1}$11) scans near $K\sim0.17$ are from aluminum powder lines. The heights of the error bars correspond to twice the square root of the number of neutron counts.

short-range correlated displacements of atoms from the ideal lattice positions. The diffuse scattering intensity distribution due to the PNR in PZN-8%PT measured near the Bragg vector **G** at the wave vector $\mathbf{Q}=\mathbf{G}+\mathbf{q}$ can be written as

$$I_{\text{diff}}(\mathbf{Q}) = A\sum_i |F_{\text{diff}}^i(\mathbf{G})|^2|f_i(\mathbf{q})|^2. \quad (1)$$

Here the sum is taken over the contributions from all six possible PNR orientations, which correspond to "pancakes" in real space with six different {110} surfaces.[13] The term $|f_i(\mathbf{q})|^2$ describes the Fourier transform of the shape of the $i$th orientation ($i=1$ through 6) of the PNR, which depends only on **q**, and gives the diffuse scattering a characteristic rodlike shape in reciprocal space. A single pair of $\langle110\rangle$-oriented rods produces the butterfly shaped diffuse scattering contours around certain Bragg peaks. On the other hand, the diffuse scattering structure factor $|F_{\text{diff}}^i(\mathbf{G})|^2$ gives the relative intensity of the diffuse scattering rod near the Bragg peak represented by reciprocal lattice vector **G**. This quantity can be expressed in terms of the relative magnitudes of the atomic displacements in the unit cell (within the $i$th orientation of the PNR)

$$|F_{\text{diff}}^i(\mathbf{G})|^2 = \left|\sum_k \mathbf{Q}\cdot\vec{\xi}_\mathbf{k}^\mathbf{i}b_k\exp(-W_K)\exp(i\mathbf{G}\cdot\mathbf{R_k})\right|^2, \quad (2)$$

where $\vec{\xi}_\mathbf{k}^\mathbf{i}$ is the atomic displacement vector, $b_k$ is the neutron scattering length of atom $k$, and $R_k$ is the lattice position of the $k$th atom in the unit cell. The Debye-Waller factors $\exp(-W_K)$ can change significantly with temperature since the ions in relaxors tend to move away from their ideal lattice positions.[30,31] However, in our calculations, only the

TABLE I. Integrated diffuse scattering intensity measured around the (200), (300), and (111) Bragg peaks.

|  | (200) | (300) | (111) |
|---|---|---|---|
| $\|\mathbf{Q} \cdot \hat{\epsilon}\|^2$ | 2.0 | 4.5 | 2.0 |
| 500 K | 6.52 | 11.6 | 2.52 |
| 400 K | 10.94 | 13.2 | 3.75 |
| 300 K | 16.86 | 13.2 | 5.04 |

TABLE II. Calculated atomic displacements and relative intensities of the different modes. The numbers for the Slater mode, last mode, and the uniform shift, refer to the size of oxygen octahedral displacement. All the numbers are normalized to Pb displacements.

|  | $\delta_{Pb}$ | $\delta_{Zn,Nb}$ | $\delta_O$ | Slater | Last | Shift |
|---|---|---|---|---|---|---|
| 500 K | 1.0 | 0.30 | −0.11 | −0.24 | −0.56 | 0.69 |
| 400 K | 1.0 | 0.37 | −0.07 | −0.26 | −0.52 | 0.71 |
| 300 K | 1.0 | 0.46 | −0.02 | −0.28 | −0.47 | 0.73 |

relative ratios of Debye-Waller factor across different Bragg peaks come into play. The variation of these ratios is relatively small over the temperature range of our study and are thus neglected in the analysis presented here. Here we take the model proposed in Ref. 13 that in-plane $\langle 1\bar{1}0 \rangle$ atomic displacements can result in the rod-type diffuse scattering along {110} directions. We can therefore simplify the expression for the structure factor as

$$|F_{\text{diff}}^i(\mathbf{G})|^2 \propto |\mathbf{Q} \cdot \boldsymbol{\epsilon}_\mathbf{i}|^2 \left| \sum_k b_k \xi_k \exp(i\mathbf{G} \cdot \mathbf{R_k}) \right|^2, \qquad (3)$$

where $\boldsymbol{\epsilon}_\mathbf{i}$ is the unit vector along the polarization direction ($\langle 1\bar{1}0 \rangle$) of the $i$th orientation of the PNR.

Our measurements show that the diffuse scattering in PZN-8%PT does not change shape significantly upon ZFC below $T_C$, i.e., the structure factor $|f_i(\mathbf{q})|^2$ does not change qualitatively. The diffuse scattering distribution still consists of six $\langle 110 \rangle$-oriented rods, the widths and lengths of which may vary, reflecting changes in the sizes or magnitude of polarizations (or both) of the PNR, but these changes do not contribute to a change in the relative intensities of the diffuse scattering measured near different Bragg peaks. If measured at the same offset $\mathbf{q}$ from a given Bragg peak $\mathbf{G}$, the relative intensities of the diffuse scattering should be completely determined by the term $|F_{\text{diff}}^i(\mathbf{G})|^2$. The linear profiles shown in Figs. 1 and 2 were obtained at the same $\mathbf{q}$, thereby measuring the intensities of the "/" and "\" wings at the same offset from the respective Bragg peaks. These linear profiles are also measured at distances sufficiently far from the Bragg peaks ($q=0$) so that (i) contributions from the tails of the Bragg peaks are negligible, and (ii) the contribution from the "/" and "\" wings are well separated in $\mathbf{q}$. We can therefore compare these intensities directly. The $q$-integrated intensities of the linear profiles are shown in Table I. The $q$-integrated intensities of linear profiles around (200) and (300) include intensity contributions from both the "/" and "\" wings, both of which have the same $|\mathbf{Q} \cdot \hat{\epsilon}|^2$ factor. At the (111) peak [and ($\bar{1}$11) peak], one of the wings is absent. In order to make a direct comparison, we listed the sum of the integrated intensities measured at (111) and ($\bar{1}$11) in the last column to include the intensity of both wings.

The relative magnitudes of the atomic displacements can therefore be calculated from Eq. (3). Here we assumed that the six oxygen atoms that forms an octahedra always move as a rigid unit. The results are shown in the first three columns of Table II. All numbers are normalized to the Pb

shifts. Note that these numbers are relative, i.e., we do not know if the increase of the overall diffuse scattering intensity upon cooling is due to increasingly larger atomic displacements, a larger total PNR volume, or both. These results only provide information on how the relative displacements of the Pb, Zn(Nb), and O atoms change. However, it is clear that upon cooling both the Zn(Nb) and O atoms tend to shift in accordance with the Pb atom shifts. This indicates a more "acoustic" type shift for the PNR.

Since the PNR result from the condensation of a soft transverse optic (TO) phonon, the atomic displacements of the PNR contributing to the diffuse scattering should be consistent with the normal mode vibrational displacements associated with the TO phonon. In the lead perovskite oxides, the dominant vibrational modes are the Slater mode and last mode.[32] In the Slater mode, the $A$ site atoms (Pb) remain stationary while the $B$ site atoms (Zn/Nb) move in opposition to the oxygen octahedra. In the last mode, the $B$ site atoms and oxygen octahedra move together in opposition to the $A$ site atoms. However, in contrast to these two modes, the atomic displacements listed in Table II clearly violate the condition that the unit cell center-of-mass be preserved. Here we use the same type of analysis as was carried out in Ref. 5, which included an additional acoustic component, also known as the "uniform phase shift." The relative ratios of all modes can then be determined (see the last three columns in Table II). It is interesting to note that the "uniform phase shift" already exists at high temperatures in the paraelectric phase. Upon ZFC into the ferroelectric phase, this uniform shift increases faster than does the growth of the polarization (optic components) of the PNR. We do not yet understand the reason for this. Nevertheless, we can speculate that in the low temperature ferroelectric phase, the increasing electrostatic energy induced by the surrounding ferroelectric polar environment would lead to a larger strain field or uniform shift of the PNR.

### B. Field effects

In contrast to the ZFC case, cooling in the presence of a moderate electric field ($E=2$ kV/cm) oriented along the [111] direction changes the shape of the diffuse scattering dramatically (see Fig. 2). All of the linear profiles show a common feature whereby the "/" wing is enhanced and the "\" wing diminished compared to ZFC results. The overall change is plotted schematically in Fig. 1(b). This partial enhancement of the diffuse scattering intensity was first reported in Ref. 17 and confirmed later by room temperature
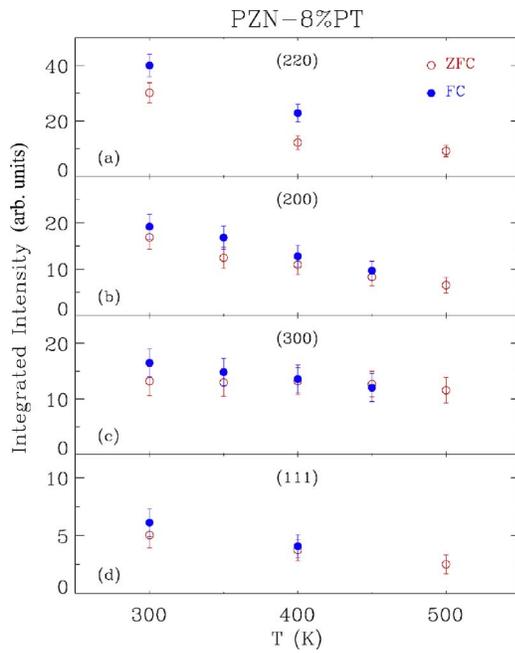
FIG. 3. (Color online) Integrated diffuse scattering intensity vs temperature measured near the (a) (220), (b) (200), (c) (300), and (d) (111) Bragg peaks. The (red) open circles represent ZFC data while the (blue) solid circles are FC data for $E = 2$ kV/cm oriented along the [111] direction.
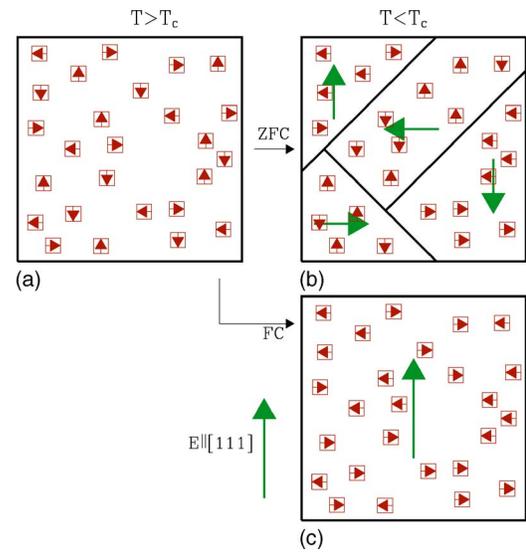


FIG. 4. (Color online) A schematic showing the PNR configurations in a relaxor system in (a) the paraelectric phase, (b) ZFC into the ferroelectric phase, and (c) FC into the ferroelectric phase. The large arrows indicate the polarization of the ferroelectric domains separated by domain walls (solid lines). The small squares represent the PNR.

electric field measurements on single crystals of pure PZN.[18] In this section we analyze the quantitative change of the diffuse scattering induced by field cooling. The integrated intensities of the linear profiles are plotted in Fig. 3. Here the intensities of both wings are included [the numbers around the (111) peak are actually the sums of the "\" wing at the (111) peak and the "/" wing at the ($\bar{1}$11) peak, as was done for Table I]. We find that the $q$-integrated diffuse intensities of both wings increase monotonically with cooling, whether ZFC or FC. The difference between the integrated intensities in the ZFC and FC cases are relatively small, considering the size of the error bars. This demonstrates that there is very likely a redistribution of the diffuse scattering intensity among the different ⟨110⟩-oriented diffuse rods, which must be associated with a redistribution of the PNR with different orientations or polarizations.

A slight enhancement of the FC linear integrated intensity compared to the ZFC case is also observed, as shown in Fig. 3. Considering previous reports of a field-induced suppression of the diffuse scattering intensities measured transverse to the Bragg wave vector in both PMN and PZN-8%PT,[15,16] it is possible that the shape of each individual ⟨110⟩ diffuse rod is also slightly affected by the field. Therefore measurements at different distances away from the Bragg peaks may lead to slightly different results. However, in general we find that the diffuse scattering in PZN-8%PT still consists of ⟨110⟩ rods upon FC, and that the intensities are mostly redistributed between different ⟨110⟩ rods, instead of within an individual rod.

On the other hand, it is quite intriguing to note that the enhanced "/" wing comes from those PNR having polariza-

tions (along [1$\bar{1}$0] and [10$\bar{1}$] perpendicular to the [111] field direction. This goes against the natural expectation that the field should be able to "align" the PNR to point along the field direction. The same behavior was also observed in a room temperature "poling" experiment performed on a single crystal of PZN using a [111] field.[18] Evidently, the energy of the PNR alone in the electric field does not favor such a configuration. This suggests that the interaction between the PNR and the surrounding lattice must also be taken into account. In the paraelectric state the PNR are randomly oriented along one of six ⟨110⟩ directions [see Fig. 4(a)]. Below the ferroelectric phase transition, macroscopic ferroelectric domains form and the cubic symmetry is broken. Thus PNR polarized along the six ⟨110⟩ directions are no longer equivalent. After cooling in zero field the polarizations of the macroscopic ferroelectric domains are randomly distributed along any of the four ⟨111⟩ directions such that there is no macroscopic preferred ⟨110⟩ polarization of the PNR, as described schematically in Fig. 4(b). However, cooling in field with $E$ applied along [111] greatly enhances the volume of the [111] polarized ferroelectric domain [Fig. 4(c)]. Our current results are consistent with the room temperature [111] field poling measurements on PZN. Both exhibit an alignment of the ferroelectric domains, instead of the PNR themselves, due to the external electric field. Our data show that those PNR with polarizations perpendicular to the field, and therefore perpendicular to the polarization of the domain in which they reside, are enhanced. This may in fact imply that these PNR are the preferred configuration in the ferroelectric phase transition. The application of a [111] field rearranges ferroelectric domains, which in turn reveals this underlying bias of the PNR macroscopically.

## IV. CONCLUSIONS

Our diffuse scattering measurements on PZN-8%PT suggest that PNR persist into the low temperature ferroelectric phase under both ZFC and FC conditions. This is consistent with previous diffuse scattering measurements as well as Raman results[33–35] obtained on other relaxor systems. We show that local atomic displacements contributing to the diffuse scattering consist of both an acoustic (strain) and optic (polar) component. This provides convincing evidence of the "polar" nature of these local orders, and stands against the argument that diffuse scatterings in relaxor systems are mainly due to local strain fields instead of local polarizations. In addition, the acoustic component, or the "uniform phase shift" of the PNR increases faster than do the polarizations upon ZFC, suggesting a build-up of strain deformation upon cooling into the ferroelectric phase.

Our FC results reveal that the preferred configuration of the PNR in the ferroelectric phase is such that the PNR tend to align perpendicular to the polarization of the surrounding ferroelectric polar domain. Although we do not fully understand the origin of this unusual configuration at this time, we speculate that the difference in the polarizations (between the PNR and the ferroelectric lattice), and large local strain deformations are probably the two most important factors that help to preserve the coexistence of PNR and the long range polar order in the ferroelectric phase. On the other hand, with both short-range polar order in the PNR and long-range ferroelectric order in the lattice developing at the same time (upon cooling), the strain caused by this mismatch will increase, resulting in an enhancement of the acoustic component of the local atomic displacements.

The coexistence of the short-range polar order of the PNR and the long-range ferroelectric order of the ferroelectric phase is quite subtle. It can be affected by many factors such as electric fields—where we believe a strong enough field should be able to eventually directly affect the PNR; pressure—which appears to be able to suppress the diffuse scattering from PMN (Ref. 36) and PZN (Ref. 37); and doping with PT—which eventually changes the structure of the low temperature phase and inevitably affects the PNR. These are interesting future topics that will require more detailed quantitative study, and which will be challenging and important.

[1] S.-E. Park and T. R. Shrout, J. Appl. Phys. **82**, 1804 (1997).

[2] G. Burns and F. H. Dacol, Phys. Rev. B **28**, 2527 (1983).

[3] L. E. Cross, Ferroelectrics **76**, 241 (1987).

[4] S. B. Vakhrushev, A. A. Naberezhnov, N. M. Okuneva, and B. N. Savenko, Phys. Solid State **37**, 1993 (1995).

[5] K. Hirota, Z.-G. Ye, S. Wakimoto, P. M. Gehring, and G. Shirane, Phys. Rev. B **65**, 104105 (2002).

[6] G. Xu, G. Shirane, J. R. D. Copley, and P. M. Gehring, Phys. Rev. B **69**, 064112 (2004).

[7] H. Hiraka, S.-H. Lee, P. M. Gehring, G. Xu, and G. Shirane, Phys. Rev. B **70**, 184105 (2004).

[8] J. Hlinka, S. Kamba, J. Petzelt, J. Kulda, C. A. Randall, and S. J. Zhang, J. Phys.: Condens. Matter **15**, 4249 (2003).

[9] B. Dkhil, J. M. Kiat, G. Calvarin, G. Baldinozzi, S. B. Vakhrushev, and E. Suard, Phys. Rev. B **65**, 024104 (2001).

[10] H. You and Q. M. Zhang, Phys. Rev. Lett. **79**, 3950 (1997).

[11] N. Takesue, Y. Fujii, and H. You, Phys. Rev. B **64**, 184112 (2001).

[12] I.-K. Jeong, T. W. Darling, J. K. Lee, T. Proffen, R. H. Heffner, J. S. Park, K. S. Hong, W. Dmowski, and T. Egami, Phys. Rev. Lett. **94**, 147602 (2005).

[13] G. Xu, Z. Zhong, H. Hiraka, and G. Shirane, Phys. Rev. B **70**, 174109 (2004).

[14] C. Stock, R. J. Birgeneau, S. Wakimoto, J. S. Gardner, W. Chen, Z.-G. Ye, and G. Shirane, Phys. Rev. B **69**, 094104 (2004).

[15] S. B. Vakhrushev, A. A. Naberezhnov, N. M. Okuneva, and B. N. Savenko, Phys. Solid State **40**, 1728 (1998).

[16] P. M. Gehring, K. Ohwada, and G. Shirane, Phys. Rev. B **70**, 014110 (2004).

[17] G. Xu, P. M. Gehring, and G. Shirane, Phys. Rev. B **72**, 214106 (2005).

[18] G. Xu, Z. Zhong, Y. Bing, Z.-G. Ye, and G. Shirane, Nat. Mater. **5**, 134 (2006).

[19] G. Xu, Z. Zhong, Y. Bing, Z.-G. Ye, C. Stock, and G. Shirane, Phys. Rev. B **67**, 104102 (2003).

[20] G. Xu, Z. Zhong, Y. Bing, Z.-G. Ye, C. Stock, and G. Shirane, Phys. Rev. B **70**, 064107 (2004).

[21] P. Bonneau, P. Garnier, E. Husson, and A. Morell, Mater. Res. Bull. **24**, 201 (1989).

[22] N. de Mathan, E. Husson, G. Calvarin, J. R. Gavarri, A. W. Hewat, and A. Morell, J. Phys.: Condens. Matter **3**, 8159 (1991).

[23] Z.-G. Ye, Y. Bing, J. Gao, A. A. Bokov, P. Stephens, B. Noheda, and G. Shirane, Phys. Rev. B **67**, 104104 (2003).

[24] J. Kuwata, K. Uchino, and S. Nomura, Ferroelectrics **37**, 579 (1981).

[25] B. Noheda, D. E. Cox, G. Shirane, J. Gao, and Z.-G. Ye, Phys. Rev. B **66**, 054104 (2002).

[26] D. La-Orauttapong, B. Noheda, Z.-G. Ye, P. M. Gehring, J. Toulouse, D. E. Cox, and G. Shirane, Phys. Rev. B **65**, 144101 (2002).

[27] Z. Feng, Z. Zhao, and H. Luo, J. Phys.: Condens. Matter **16**, 6771 (2004).

[28] H. Ohwa, M. Iwata, H. Orihara, N. Ysauda, and Y. Ishibashi, J. Phys. Soc. Jpn. **70**, 3149 (2001).

[29] H. Hiraka (private communications).

[30] R. Pirc and R. Blinc, Phys. Rev. B **60**, 13470 (1999).

[31] A. A. Bokov and Z.-G. Ye, J. Mater. Sci. **41**, 31 (2006).

[32] J. Harada, J. D. Axe, and G. Shirane, Acta Crystallogr., Sect. A: Cryst. Phys., Diffr., Theor. Gen. Crystallogr. **26**, 608 (1970).

[33] J. Toulouse, P. DiAntonio, B. E. Vugmeister, X. M. Wang, and L. A. Knauss, Phys. Rev. Lett. **68**, 232 (1992).

[34] B. E. Vugmeister, P. DiAntonio, and J. Toulouse, Phys. Rev. Lett. **75**, 1646 (1995).

[35] P. DiAntonio, B. E. Vugmeister, J. Toulouse, and L. A. Boatner, Phys. Rev. B **47**, 5629 (1993).

[36] B. Chaabane, J. Kreisel, B. Dkhil, P. Bouvier, and M. Mezouar, Phys. Rev. Lett. **90**, 257601 (2003).

[37] M. Ahart, R. E. Cohen, V. Struzhkin, E. Gregoryanz, D. Rytz, S. A. Prosandeev, Ho-kwang Mao, and R. J. Hemley, Phys. Rev. B **71**, 144102 (2005).